Title
Quantification of breast lesion compositions using low-dose spectral mammography: A feasibility study

Journal
Medical Physics, 43(10)

ISSN
0094-2405

Authors
Ding, Huanjun
Sennung, David
Cho, Hyo-Min
et al.

Publication Date
2016-09-19

DOI
10.1118/1.4962481

Peer reviewed

Quantification of breast lesion compositions using low-dose spectral mammography: A feasibility study

Huanjun Ding, David Sennung, Hyo-Min Cho, and Sabee Molloi[a)]
Department of Radiological Sciences, University of California, Irvine, California 92697

(Received 27 January 2016; revised 23 August 2016; accepted for publication 29 August 2016; published 19 September 2016)

Purpose: The positive predictive power for malignancy can potentially be improved, if the chemical compositions of suspicious breast lesions can be reliably measured in screening mammography. The purpose of this study is to investigate the feasibility of quantifying breast lesion composition, in terms of water and lipid contents, with spectral mammography.
Methods: Phantom and tissue samples were imaged with a spectral mammography system based on silicon-strip photon-counting detectors. Dual-energy calibration was performed for material decomposition, using plastic water and adipose-equivalent phantoms as the basis materials. The step wedge calibration phantom consisted of 20 calibration configurations, which ranged from 2 to 8 cm in thickness and from 0% to 100% in plastic water density. A nonlinear rational fitting function was used in dual-energy calibration of the imaging system. Breast lesion phantoms, made from various combinations of plastic water and adipose-equivalent disks, were embedded in a breast mammography phantom with a heterogeneous background pattern. Lesion phantoms with water densities ranging from 0% to 100% were placed at different locations of the heterogeneous background phantom. The water density in the lesion phantoms was measured using dual-energy material decomposition. The thickness and density of the background phantom were varied to test the accuracy of the decomposition technique in different configurations. In addition, an *in vitro* study was also performed using mixtures of lean and fat bovine tissue of 25%, 50%, and 80% lean weight percentages as the background. Lesions were simulated by using breast lesion phantoms, as well as small bovine tissue samples, composed of carefully weighed lean and fat bovine tissues. The water densities in tissue samples were measured using spectral mammography and compared to measurement using chemical decomposition of the tissue.
Results: The thickness of measured and known water contents was compared for various lesion configurations. There was a good linear correlation between the measured and the known values. The root-mean-square errors in water thickness measurements were 0.3 and 0.2 mm for the plastic phantom and bovine tissue backgrounds, respectively.
Conclusions: The results indicate that spectral mammography can be used to accurately characterize breast lesion composition in terms of their equivalent water and lipid contents. © *2016 American Association of Physicists in Medicine.* [http://dx.doi.org/10.1118/1.4962481]

Key words: dual-energy, mammography, material decomposition

1. INTRODUCTION

Currently, the standard imaging modality for breast cancer screening is mammography.[1–5] Yet despite mammography's impressive advantages in detection performance, imaging time, and cost-effectiveness, its limitations are widely recognized.[6] One of the biggest challenges for accurate early detection in breast cancer screening is increasing the specificity of tumor detection to avoid recalling healthy women and exposing them to follow-up examinations that may involve additional radiation or a needle biopsy, which not only increases the healthcare cost but also adds risk and patient discomfort.[7,8] With conventional mammograms, the radiologist makes the determination based on specific features in mammographic patterns such as shape, size, margin, or pattern of abnormal density.[9,10] However, in many cases, it can be difficult to characterize a suspicious lesion as benign or malignant based only on its mammographic appearance. Thus, a follow-up examination is required.[11]

A recent report suggests that in addition to irregular mass shape, spiculated mass margin, and patient age, a high mammographic attenuation of a mass increases its likelihood of malignancy.[11] However, high mass density by itself is not sufficiently accurate to avert the need for a biopsy. The predictive capability could potentially be improved if lesions could be characterized quantitatively according to their chemical composition. Thus, there is increased interest in developing lesion characterization techniques that can characterize lesions as benign or malignant during the initial screening. It has been suggested that malignant tumors have reduced lipid and increased water contents compared to normal breast tissue.[12–15] In addition, other reports suggest a positive correlation between increased tissue water content and carcinogenesis.[16] X-ray linear attenuation coefficients of breast lesions have been studied in the past, and were reported to be different from fibro-glandular tissue, especially in the low energy range.[17,18] A recent study also suggested that the

attenuation of cyst fluid was found to be significantly different from that of water.[19] These reports indicate that mammography's sensitivity and specificity may be improved if breast tissue composition can be accurately measured to improve characterization of lesions according to their composition.

Dual-energy imaging can exploit differences between specific types of breast tissues due to their unique effective atomic numbers (Z), providing separate quantitative thickness measurements for each tissue. This technique has been successfully implemented for breast density quantification by using the standard screening mammogram as the low-energy image and an additional low-dose high-energy image.[20–22] However, the high-energy image may slightly increase the mean glandular dose and result in misregistration artifacts due to patient motion. These potential challenges have been successfully addressed with the recent developments in photon-counting x-ray detectors. A spectral mammography system based on photon-counting detectors in a scanning multislit geometry[23] allows dual-energy data acquisition to be completed with a single exposure. A user-defined energy threshold is used to sort photons into low-energy and high-energy bins, according to their energies. Compared to traditional dual-kVp technique, energy-resolved photon-counting detectors minimize the spectral overlap and completely eliminate the misregistration artifacts in dual-energy decomposition. In addition, conventional charge-integrating detectors generally work in the current mode, which integrates both the signal and noise from the detector and electronics over time. The presence of electronic noise can substantially reduce the signal-to-noise ratio (SNR) in low-dose imaging.[24] On the other hand, photon-counting detectors can eliminate electronic noise, which offers promising potential for low-dose imaging.[25] A previous report shows that an ideal photon-counting detector with good energy resolution outperforms conventional charge-integrating detectors in image quality and various detection tasks.[26] It has been shown that the photon-counting spectral mammography system can accurately measure glandular and adipose tissue thicknesses for breast density quantification.[27] Thus, it is of interest to investigate the feasibility of characterizing breast lesion composition using dual-energy decomposition of spectral mammography images acquired on a photon-counting system.

The fundamental chemical components in either normal or cancerous breast tissues are water, lipid, and protein. Previous reports have characterized breast tissue into water, lipid, and protein contents using dual-energy mammography.[28,29] They suggested that the knowledge of breast lesion composition appeared additive in combination with existing diagnostic methods for the distinction between different benign and malignant lesion types.[29] However, the results failed to reach statistical significance. One potential issue of using a three-component model with dual-energy mammography is that it requires accurate breast thickness measurement as the third independent physical measurement. Unfortunately, this is difficult to obtain in practice, particularly in the periphery of the breast where the breast is not in contact with the compression plate. Uncertainties in thickness estimation, induced by the shape model and the mechanical precision of the compression paddle, can lead to significant errors in lesion compositional analysis,[30] which may reduce the predictive power for malignancy. To address this potential issue, we propose to characterize breast lesions with a two-compartment model using water and lipid as the basis materials. Our previous postmortem study showed that protein generally contributed less than 6% to the mass of normal breast tissue.[31] More importantly, using a two-compartment model, protein in breast tissue will be decomposed into water and lipid basis materials. Since the dual-energy decomposition coefficients are well defined for the two basis materials, the presence of a small amount of protein will only add a small systematic offset in the estimation of water and lipid contents. This approach has been tested in a simulation study.[32] Dual-energy signals from simulated breast tissues, which were composed of water, lipid, and protein contents, were generated using a previously reported simulation package.[27] The chemical compositions of the simulated breast tissues were designed to match the experimental results from a previous postmortem breast study.[31] The simulated dual-energy signals were then decomposed into water and lipid thickness signals. The result showed that the measured water content using a two-compartment model correlated strongly (Pearson's $r > 0.99$) with the known water content in breast tissue with a linear correlation slope of 1.05 and an offset of 0.1 mm. In this paper, we investigate the feasibility of characterizing breast lesions using a two-compartment model with physical phantoms and tissue samples. The purpose of this study is to evaluate the accuracy and precision of dual-energy decomposition for lesion characterization.

2. MATERIALS AND METHODS

2.A. Spectral mammography system

A spectral mammography system (MircoDose SI L50, Philips, Inc.) was used during the studies, which is able to acquire dual-energy images within a single exposure. The system consists of a tungsten-anode x-ray tube, an Al filter, a precollimator, a postcollimator, and the Si-strip photon-counting detector unit, which are all mounted on a common arm that can rotate around the center of the source, allowing the collimators and the photon counting detector to scan relative to the compressed breast. The detector's energy resolution at the mammography energy range is approximately 5 keV at full width half maximum (FWHM).[33] The electronic readout noise is effectively eliminated by selecting an appropriate background threshold. A multislit collimator shapes the beam to match the detector, and a two-dimensional image is generated when the beam and detector are scanned relative to the breast. The scanning multislit technique helps to eliminate the scattered radiation, which further improves the SNR. A previous study suggests that the scatter to primary ratio (SPR) for this geometry is expected to be less than 6% for phantom thicknesses ranging from 3 to 7 cm at various tube voltages.[34] More details about the spectral mammography system can be found in a previous publication.[27]

2.B. Dual-energy calibration

A calibration phantom consisting of two compartments, made from Plastic Water® LR and adipose equivalent plastics (CIRS, Norfolk, VA), was constructed for dual-energy decomposition. The x-ray attenuation coefficients of plastic water were calculated based on its elemental compositions provided by the manufacturer and were found to closely resemble those of pure liquid water in the mammographic energy range, which provides a reason for the use of solid water as a substitute for liquid water in the dual-energy calibration. Unfortunately, it is difficult to fabricate a plastic-based lipid phantom that can represent real lipid. Instead, we use the adipose equivalent phantom which consists of approximately 15% water and 85% lipid, according to its chemical composition.[35] After dual-energy decomposition by using plastic water and adipose as the basis materials, a linear transformation can be applied to convert the basis material into water and lipid based on the calibrated composition of the adipose equivalent phantom.[19] A schematic drawing of the calibration phantom is shown in Fig. 1. It had a stair shape with four different heights: 2, 4, 6, and 8 cm, where each of the heights had five different plastic water densities ranged from 0% to 100% with an increasing step of 25%. This design provided a total of 20 calibration points that cover both thickness and density variations. The calibration phantom was carefully machined and the thickness of each step was confirmed with caliper measurements, which suggested an uncertainty of approximately 25 μm. The calibration phantom was imaged at all the available tube voltages on the system, including 26, 29, 32, 35, and 38 kVp. The spectral mammography system has a built-in calibration for the selection of the high energy threshold, which depends on the tube voltage and phantom thickness. The log-signals from the low-energy and high-energy images were derived for all 20 calibration points.

In dual-energy decomposition, the low-energy and high-energy signals of a tissue with given thickness can be written as a linear combination of the two basis materials used in the calibration.[20] The two measurements from different energy bins provide enough information to solve for the thickness of the two basis materials. Due to the polyenergetic nature of the diagnostic x-ray spectra, dual-energy imaging usually uses higher-order inverse functions that map the log-signals into content thicknesses. In this study, a nonlinear rational fitting function was used, which has been shown to have high fitting accuracy,[36] to calibrate the imaging system

$$t = \frac{a_0 + a_1 S_L + a_2 S_H + a_3 {S_L}^2 + a_4 S_H S_L + a_5 {S_H}^2 + a_6 {S_L}^3 + a_7 {S_H}^3}{1 + b_1 S_L + b_2 S_H + b_3 {S_L}^2 + b_4 {S_H}^2}. \quad (1)$$

The calibration process will substitute the known thickness values, t_i, for either plastic water or adipose equivalent phantoms, and the corresponding dual-energy attenuation measurements S_L and S_H into Eq. (1). Subsequently, the system calibration parameters (a_0, a_1, ...) for each material will be determined separately from a nonlinear least-squares minimization algorithm.[37] Using the measured dual-energy log-signals, the calibration parameters will then be used as the decomposition coefficients to characterize lesions in terms of water and lipid contents. This method has been previously validated in dual-energy breast density quantification studies, which has shown good accuracy for tissue compositional analysis.[27]

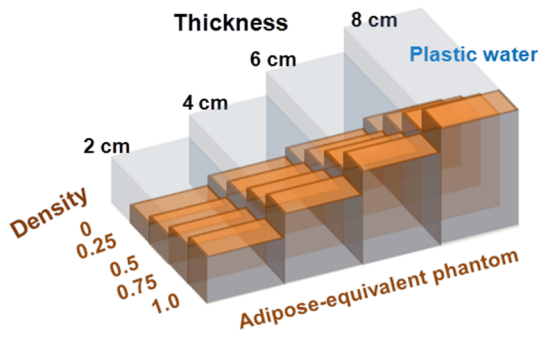

FIG. 1. A schematic drawing of the calibration phantom composed of plastic water and adipose equivalent material of various thicknesses and densities.

2.C. Phantom and tissue validation

To validate the proposed method, phantom studies were designed using a mammographic phantom with a heterogeneous pattern (BR3D, CIRS, Norfolk, VA) as the background in order to simulate the anatomical noise in clinical mammograms. The BR3D phantom is constructed with a swirled pattern of adipose and glandular tissue equivalent materials with an overall 50:50 ratio. The random swirling pattern makes the background different depending on the position on the phantom, which leads to variations of the local glandularity. The lesion phantoms were made from plastic water and adipose disks that are 1 mm in thickness and 2 cm in diameter. Five of those disks were stacked together in order to simulate a 0.5 cm lesion. The configuration of the lesion disk phantoms were varied to produce six possible plastic water densities, which ranged from 0% to 100% with an increasing step of 20%. As a feasibility study, the size of the phantom was designed to simulate the largest dimension of an average lesion observed in mammography,[38] so that the compositional characterization will not be limited by quantum noise. The uncertainty in the thickness estimation of the disk phantoms was approximately 25 μm. To embed the lesion disk phantoms

in the breast background, a 0.5 cm thick adipose slab containing two holes 2 cm in diameter was used to hold the lesion disks. The adipose slab with the embedded lesion phantoms was then placed on top of the BR3D phantoms, which forms a breast phantom that has a uniform thickness around the lesions. This phantom design approximately resembles a breast under the paddle compression in clinical mammography scans.

Four phantom validation studies were designed, which addressed the effects of anatomical noise, breast thickness, breast density, and lesion depth. The first study imaged the lesion phantoms of various water densities on different background phantoms. A uniform 4 cm adipose-equivalent slab was used to simulate a homogeneous breast background without the presence of anatomical noise. BR3D phantom with a total thickness of 4 cm was used to produce a heterogeneous background, which simulates the anatomical noise. Lesions were placed on top of the BR3D background at random locations that were at least a few centimeters away from each other. This approach allowed us to vary the local glanularity for each lesion phantom, so that the effect of a heterogeneous background on lesion compositional measurements could be assessed. The second study fixed the water density of the lesion phantom at 40% and imaged it on BR3D phantoms of different thicknesses ranging from 2 to 5 cm. The third study used the same 40% water density lesion phantom, but imaged it with a series of uniform glandular and adipose tissue equivalent slabs (CIRS, Norfolk, VA) of a total of 4 cm. The combination of the uniform and BR3D phantoms was used to provide a set of breast backgrounds of different densities ranging from 0% to 100%. Finally, the last phantom study inserted the 40% water density lesion phantom into different levels of a 5 cm BR3D phantom, which simulated different locations of a lesion in the projection direction.

To further test the lesion characterization method in tissue, an *in vitro* study was designed using bovine tissue as the background. Pure lean and fat bovine tissue pieces were mixed together to form heterogeneous background phantoms of 25%, 50%, and 80% lean weight percentages. The mixture of bovine tissue samples was kept in thin, plastic bags and shaped to resemble compressed breasts. The lesion disk phantoms of various water densities were placed inside the tissue background and imaged at different locations. In addition, small volumes of lean and fatty tissues were carefully weighed to produce various lesion phantoms with a lean mass percentage ranging from 0% to 100%. The tissue lesion phantoms were placed in a plastic tube with a diameter of 10 mm. The total height of the tissue phantoms were approximately 10 mm. This setup helped to fix the shape of the lesion phantoms and also allowed us to keep track of the locations in the tissue background. After imaging, all tissue lesion phantoms were decomposed into water, lipid, and protein using a previously developed chemical analysis process. Details of the chemical analysis steps have previously been reported.[31] The measured weight of water, lipid, and protein contents was converted into volumes using the corresponding density values. Volumetric densities were calculated for water as the reference standard.

2.D. Image processing

Automatic exposure mode was used for all data acquisition, where the exposure was optimized according to the tube voltage and phantom thickness based on the built-in system calibration. The mean glandular dose for a single exposure ranged from 0.2 to 0.8 mGy, depending on the imaging parameters and phantom thickness. Dual-energy images in the raw format generated from the spectral mammography system were first normalized by the corresponding open field images at the same tube voltage settings. Then, the log signals were calculated for both low-energy and high-energy images and were used for material decomposition using Eq. (1) with the calibrated decomposition coefficients for plastic water and adipose. The decomposition process converted the low-energy and high-energy log signal images into thickness images of the two basis materials, where the pixel values represent the total plastic water/adipose thickness. In the case where a lesion phantom is inside this volume, the decomposed plastic water signal can then be written as the sum of the plastic water thickness in the lesion and in the background above and below the lesion. The lesion's plastic water content can then be isolated by subtracting the total decomposed signal from a region outside the lesion, under the assumption that the plastic water content distribution in the background is locally uniform in a region that has a similar size as the lesion. Thus, the subtracted signals can be used to characterize lesions with different chemical compositions in terms of plastic water and adipose contents.

To measure the signal difference between the lesion and the surrounding area, two ROIs were manually delineated on the dual-energy decomposed images. A circular ROI was used to measure the decomposed material thicknesses inside the disks. An annular ROI with a width of 1 mm was used to measure the thickness signal from an adjacent area near the lesion phantoms. The two ROIs were separated by a narrow region with a thickness of approximately 1 mm, in order to avoid any potential blurring induced by magnification. A schematic illustration of the ROI selections is shown in Fig. 2. The signal difference for plastic water thickness measured on dual-energy decomposed image was compared to the known values for all lesion phantoms. Linear regression analysis was performed for all validation studies. Root-mean-square (RMS) error and standard error of the estimate (SEE) were used to characterize the accuracy and the precision of the measurements, respectively. In the tissue lesion analysis, an additional step was taken to convert the measured plastic water and adipose phantom thicknesses into water and lipid thicknesses. Linear regression analysis was performed to investigate the correlation of water densities obtained through spectral mammography and chemical analysis.

3. RESULTS

Figure 2 shows an example of the images acquired during the phantom validation. In the dual-energy images [Figs. 2(a) and 2(b)], lesion disks of 80% water density can be seen embedded within a swirled background produced by the BR3D

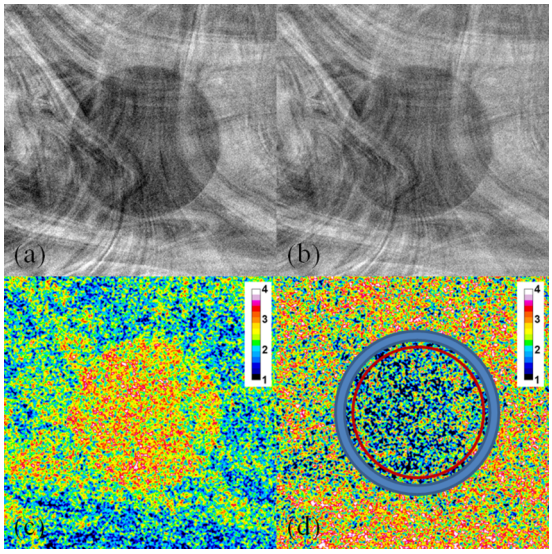

FIG. 2. Low-energy (a) and high-energy (b) images in the raw format for an 80% water density lesion embedded in a 4 cm BR3D breast phantom, and the decomposed plastic water (c) and adipose (d) images. The colored scales are in unit of cm. A schematic illustration of the circular and the annular ROIs used to derive the thickness differences is shown in (d).

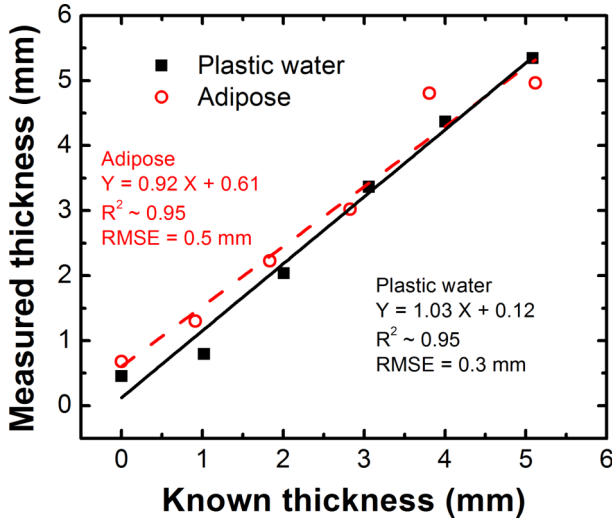

FIG. 3. Measured plastic water and adipose thicknesses in lesion phantoms of different densities as a function of the known values for a 4 cm heterogeneous BR3D phantom. Lines of best fit are shown for the corresponding components of plastic water (solid) and adipose (dashed).

breast phantom. After decomposition, the thickness of plastic water and adipose above each pixel is presented in Figs. 2(c) and 2(d), respectively. Although the current decomposition approach will not minimize the background noise induced by the swirl pattern, its focus is to quantify the compositional thicknesses in different regions of the phantom. In a clinical application, this method will be used to measure lesion composition in the presence of anatomical noise.

In the first validation study, lesion disk phantoms of various water densities were imaged on uniform adipose slabs. The measured plastic water thicknesses agreed well with the known values with a RMS error of 0.2 mm. The slope and the offset from a linear regression analysis were derived to be 1.02 and 0.2 mm. Then, the lesion phantoms were imaged with a 4 cm BR3D breast phantom, which represents an average breast compression thickness in mammography.[39] Plastic water thickness of the lesion measured using the method described above (see Sec. 2.D) was compared to the known thickness of the plastic water disks shown in Fig. 3. The results showed a good linear correlation between the measured and the known thicknesses of the decomposed compartments for both plastic water and adipose. The slopes of the best linear fitting lines were derived to be 1.03 and 0.92 for plastic water and adipose, respectively. The linear correlation coefficient (R^2) was determined to be 0.95 for both basis materials. The RMS errors were estimated to be 0.3 and 0.5 mm for plastic water and adipose, respectively.

Since the method to characterize lesion compositions depends on the subtraction of the normal surrounding tissue component thickness, it is necessary to investigate the effect of the background thickness and density variations on the accuracy of the thickness quantification. In Fig. 4, the measured plastic water and adipose thicknesses in a 40% water density lesion phantom are shown as a function of the background breast phantom thicknesses, which ranged from 2 to 5 cm. The expected thickness values for the two components are shown as dashed lines in the figure. It can be seen that the errors in lesion characterization are independent of breast thickness. The RMS errors over all breast thicknesses were determined to be 0.2 and 0.3 mm for plastic water and adipose, respectively. The mean and standard deviation for plastic water density measurements were 40.5% and 5.1%, respectively. It should be noted that when the background thickness was varied by adding BR3D slab phantoms, the local glandularity was altered as well. Some measurements may result in slightly higher errors than others due to the rapid change of background glandularity, which deteriorates our initial assumption that the composition of the background is locally uniform around the lesion phantom. The effect of breast density on lesion characterization accuracy is shown in Fig. 5. The same 40%

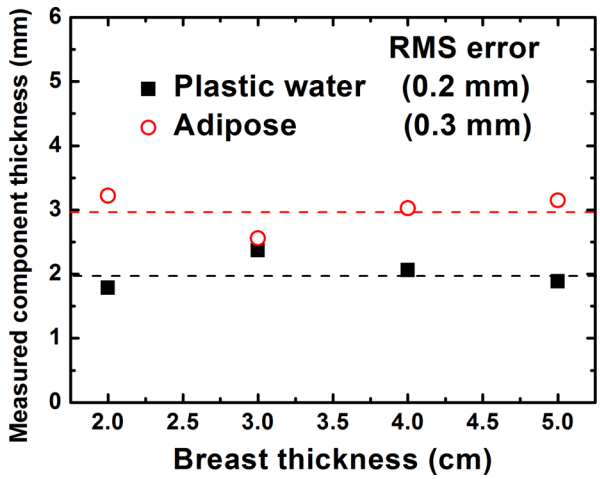

FIG. 4. Compositional measurements of a 40% water density lesion in breast phantoms of different thicknesses. The dashed lines indicate the known thicknesses of plastic water and adipose phantom.

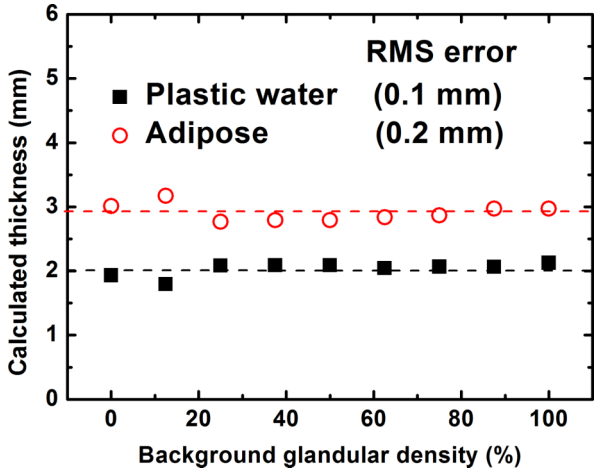

FIG. 5. Compositional measurements of a 40% water density lesion in breast phantoms of different glandularities. The dashed lines indicate the known thicknesses of plastic water and adipose phantom.

water density lesion was imaged with uniform breast phantoms of various glandularities. Similar to the breast thickness study, the measured thicknesses aligned tightly around the expected values. The RMS errors are 0.1 and 0.2 mm for plastic water and adipose, respectively. The mean and standard deviation for plastic water density measurements were 40.6% and 2.1%, respectively. This result indicated that change in breast density does not affect the measurement accuracy for lesion characterization using the proposed method.

Due to the projection nature of mammography, the position of the lesion inside the breast may affect the magnification of the lesion. The decomposition results of a 40% water density lesion imaged at different positions inside a 5 cm BR3D breast phantom are shown in Fig. 6. The calculated RMS errors in thicknesses of the decomposed plastic water and adipose were 0.2 and 0.3 mm, respectively. The mean and standard deviation for plastic water density measurements were 37.5% and 5.5%, respectively. Thus, it can be seen that the accuracy

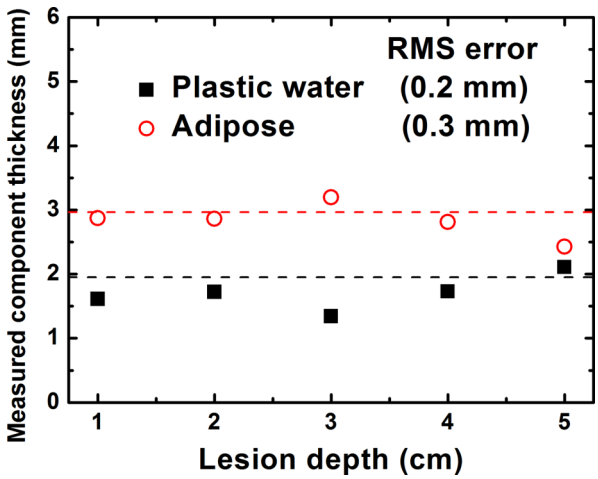

FIG. 6. Compositional measurements of a 40% water density lesion that was inserted at different depths within a 5 cm thick BR3D background phantom. The dashed lines indicate the known thicknesses of plastic water and adipose phantom.

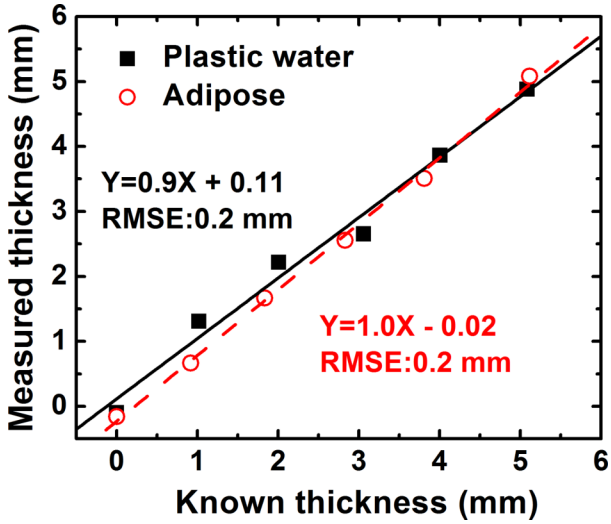

FIG. 7. Measured thicknesses of the decomposed plastic water and adipose as a function of the known values in lesion phantoms, which were embedded in a bovine tissue background. Lines of best fit are shown for the corresponding components of plastic water (solid) and adipose (dashed).

of the investigated lesion characterization is not affected by the location of the lesion inside the breast.

Finally, the result of lesion characterization in a bovine tissue background is shown in Fig. 7. There is a good correlation between the calculated thickness of the decomposed materials and the known values of the disk thicknesses. In a linear regression analysis, the correlation slopes for plastic water and adipose were derived to be 0.93 and 1.01, respectively. The linear correlation coefficients (R^2) for the two components were 0.98 and 0.99. RMS errors for both plastic water and adipose were estimated to be 0.2 mm. When using bovine tissue lesion phantoms with tissue background, a good linear correlation between the decomposed water density and the reference standard from chemical analysis was observed, as shown in Fig. 8. The correlation coefficient (R^2) was estimated to be 0.96. Linear regression analysis resulted in a slope

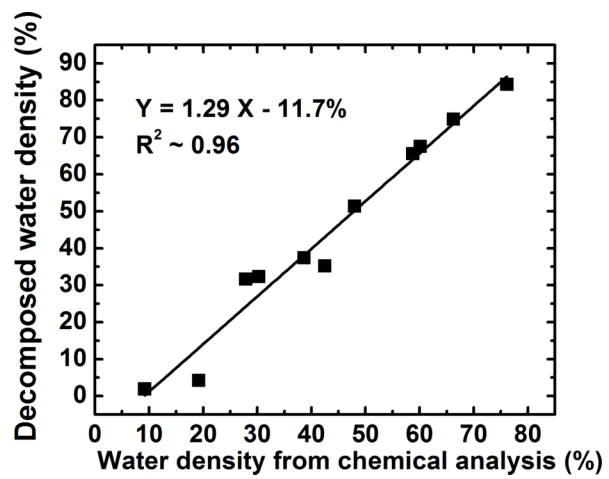

FIG. 8. Decomposed water density from spectral mammography as a function of that obtained from chemical analysis for bovine lesions embedded in a bovine tissue background. Line of best fit is also shown in the plot.

TABLE I. Summary of water density measurements for lesions with various backgrounds.

	Uniform	BR3D	Bovine tissue	Tissue lesion
Slope	1.02	1.03	0.93	1.29
Offset (%)	3.3	2.5	2.3	−11.7
R^2	0.99	0.95	0.98	0.96
RMS error (%)	4.2	6.1	4.9	7.4
SEE (%)	1.3	4.5	4.1	4.6

of 1.29 and an offset of −11.7%. To compare the accuracy and precision of lesion characterization with different types of background, the results on water density measurements from all validation studies are summarized in Table I. The first three columns of data were derived from the plastic disk lesion phantoms with different backgrounds, and the last set of data was derived from the bovine tissue lesion phantoms imaged with the bovine tissue background. Water density, instead of thickness, was used in the comparison, since the chemical analysis of tissue lesion phantoms can only generate volumetric information for water density calculations. Water densities of the plastic lesion phantoms were derived using the ratio of measured water thickness to the total lesion thickness.

4. DISCUSSIONS

This study investigates the feasibility of measuring breast lesion composition in terms of water and lipid by using low dose dual-energy mammography. It is generally understood that the attenuation of malignant lesions is different from that of fibro-glandular breast tissue at mammographic energy range due to their higher water content.[17,18,40] However, the chemical composition of benign lesions may spread in a relatively large range.[41] While some benign lesions, such as fibroadenomas, may contain relatively high amounts of water, many other types of benign lesions contain less water and more lipid as compared to malignant tumors. It is expected that the chemical composition of a lesion can potentially help differentiate malignant from benign tumors. Therefore, the proposed technique can help reduce the number of false-positives and potentially decrease the number of negative breast biopsies without additional radiation dose.

Dual-energy imaging can provide accurate quantitative thickness measurements for two basis materials without relying on any assumptions about the breast thickness. Therefore, dual-energy imaging can effectively eliminate errors induced by the shape model and the compression paddle's mechanical precision. However, it also limits the compositional analysis to two basis materials. For this reason, we have characterized the lesion composition in terms of water and lipid contents, ignoring the relatively small amount of protein in breast tissue.[31] In a previous postmortem study, we have reported that the amount of protein is highly correlated with water and lipid in breast tissue.[31] Therefore, the presence of protein in the lesion is expected to result in a systematic shift in the measured water and lipid thicknesses. One advantage of characterizing breast lesions in terms of water and lipid contents is the possibility of performing an accurate calibration, since both basis materials are easy to obtain and have minimal variations. In theory, the system calibration can be done with pure water and oil. However, both of the two basis materials are in a liquid form which makes it challenging for eventual clinical implementations. In this study, a solid plastic calibration phantom, consisting of plastic water and adipose equivalent materials, was used for the purpose of water–lipid decomposition. For future clinical applications, the decomposed basis material thicknesses can be converted into water and lipid values using a basis transfer function.[19] The plastic phantoms' exact composition, in terms of water and lipid, can be experimentally determined through an initial calibration process by using liquid water and lipid. The measured log-signal from the plastic phantoms can be mapped to the log-signals obtained for water and lipid of the same thickness. The phantom composition can then be determined using the mapping coefficients. Although such a process still involves the use of liquid, it will have to be done only one time. Once the plastic phantoms' water–lipid composition is determined, the dual-energy calibration can be carried out with plastic-based phantoms by converting the phantom thicknesses into actual water and lipid thicknesses. This is a linear transformation process which will not affect the precision of the lesions' compositional measurements.

In mammography, the measured signal is associated with the total breast thickness that the photons penetrate before getting registered in the detector, which includes signals from both the lesion and the background tissue. To be able to isolate the information from the lesion, the signal in the lesion region can be subtracted from the surrounding tissue. The assumption here is that the chemical composition of normal breast tissue inside the lesion region is the same as that in the adjacent region. Different types of background phantoms were used to evaluate the potential error induced by this assumption. In the first experimental setup, a uniform background represented an ideal case, where this assumption is perfectly satisfied. The measurement accuracy for uniform background, characterized by the RMS error, was calculated to be 4.2% (Table I), which is higher than the error in a previous breast density quantification study using large slab phantoms with uniform thickness.[27] However, the technique involved subtraction between two regions after material decomposition, which effectively increases the noise. Using a standard error propagation theory and assuming a decomposition error of 2% for both regions inside and outside the lesion,[27] the expected error in an ideal case will be approximately 2.8%. The additional error observed in this study on centimeter-sized lesions compared to a whole breast can be mostly attributed to the reduction in measurement area in both calibration and validation steps. This is not only caused by the increased quantum noise but also due to the background tissue nonuniformity. To estimate the increase in error due to a reduced measurement area, the variation in plastic water density was measured for ROIs of 0.5 and 2 cm diameter at the same location in plastic lesion phantoms on a uniform background. The variation was found to be increased in the 0.5 cm diameter ROI by approximately 0.5% as compared with the 2 cm diameter ROI.

In the second setup, a BR3D phantom with swirl pattern was used to simulate anatomical noise. The introduction of the random background noise with BR3D phantoms is essential to validate the above assumption and to understand the potential error in lesion compositional analysis. The RMS error in water density quantification with a BR3D background was derived to be 6.1% (Table I). The increased quantification error, as compared to that from a uniform background, can be used to estimate the potential error induced by the proposed method, where the chemical composition surrounding the lesion was used to estimate the composition of background inside the lesion. Furthermore, lesions were intentionally imaged at different locations on the BR3D background, so that an independent estimation of the background can be performed for each lesion. It can be seen that the precision of the measurement was significantly affected due to the presence of background noise, as the SEE increased from 1.3% to 4.5% and the coefficient of determination (R^2) decreased from 0.99 to 0.95 when BR3D background was used. It also found that the size of the annular ROI can affect the accuracy in background estimation, which can contribute to the quantification error. An initial evaluation was conducted to determine the optimal size of the background ROI with the BR3D phantom. The results showed that the decomposition error decreased monotonically as the size of the annular ROI was reduced, and it plateaued for annular ROIs less than 1.3 mm. We, therefore, used a 1 mm wide annular ROI for all the validation studies. It should be noted that the selection of the annular ROI size depends on the spatial frequency of the background noise. A similar optimization should be conducted for clinical images.

Although the BR3D phantom offers a certain type of noise structure, it is not identical to the anatomical noise in clinical images. Power spectra analysis suggested that the magnitude of the power spectra curves of the BR3D phantom was within the range of clinical images but the power law exponent (β) was lower than the average for clinical images.[42] In particular, BR3D phantom has less low frequency noise as compared to clinical images.[42] To address this issue, we introduced bovine tissue background which has been used to simulate breast tissue for breast density quantifications.[35] The mixture of bovine tissue background not only offered low frequency background noise but also helped to understand the effect of protein in the tissue. Comparing the disk lesion measurements with bovine tissue background to those with plastic phantom background, it can be seen that the accuracy (RMS error of 4.9%) was improved with respect to BR3D, but was not as good as the uniform background. The disk lesion measurements with bovine tissue background also had lower precision (SEE of 4.1%) compared to that of the uniform background.

For all the validation studies using plastic lesion disks, the calibration and decomposition basis materials were identical. This allowed a direct comparison between the decomposed thicknesses and the known values from physical measurements. Therefore, all linear regression analysis resulted in a slope very close to unity and a small offset values. As shown in Table I, the offsets for lesion disk phantoms were comparable to or much less than the RMS errors, which suggested that the offset in the linear fitting was simply induced by experimental errors. On the contrary, when bovine tissue lesion phantoms were studied, the linear regression analysis resulted in a fitting slope of 1.29 and an offset of −11.7%. This is expected, since the proposed method decomposes the measured lesion signal into two basis materials, ignoring the presence of protein. On the other hand, in chemical analysis, tissue samples were characterized in terms of water, lipid, and protein contents. In dual-energy decomposition, the signal from protein will be partly decomposed into water content, leading to higher water density estimation from spectral mammography. Based on chemical compositions of tissue, water and protein concentrations are highly correlated. Samples with higher water content will get higher signal from protein, which explains the fact that our correlation slope is larger than unity. In a simulation study, which decomposed 5 cm thick breast tissue into plastic water and adipose basis materials, the slope and offset of the linear fitting between the measured and the known plastic water densities were derived to be 1.23% and −17.1%, respectively.[32] The observed correlation in the experimental bovine tissue study was in good agreement with the simulation results. As previously indicated, the presence of protein in the background does not affect the accuracy and precision in lesion characterization. However, the protein contents presented in the lesion itself can be a major source of error when the accuracy of the method is evaluated, as evidenced by the relatively large RMS error of 7.4%. It should also be noted that although chemical analysis offers a good measure of sample composition, experimental errors, in the range of 1%–2%, may still be present for small samples, especially when the amount of water is low.[31] We observed more scattered results for low-density lesion samples, which can be partly attributed to the increased experimental error in chemical analysis. Nevertheless, we observed a good linear correlation in water density measurements between spectral mammography and chemical analysis with R^2 comparable to that from the disk phantoms (Fig. 8). More importantly, the SEE was approximately the same as the measurements based on plastic disk lesion phantoms. Thus, it is suggested that the precision of the proposed method is preserved when using only two basis materials for lesion characterization.

The study investigated the effects of breast shape and density on the accuracy of lesion characterization in terms of water and lipid. The results suggested that dual-energy decomposition measurements do not depend on breast thickness, glandularity, or lesion depth. The mean values in water density measurements were in good agreement with the known values within the range of RMS errors shown in Table I. The variation induced by breast characteristics was also comparable to the measurement precision. This suggested that the accuracy and precision will not be affected by breast shape and density.

The current study used a clinical imaging protocol that was designed for screening mammography. The high energy threshold was already optimized for breast density quantification according to a previous simulation study,[27] and is expected to offer a good SNR for lesion characterization in terms of water and lipid contents. The mean glandular dose was estimated to be 0.2–0.8 mGy using automatic exposure control, which is comparably lower than the current clinical

standard.[43] The method aims to offer a quantitative metric to characterize the chemical composition of a suspicious lesion in screening mammography without additional radiation. At the current dose level, the noise can be amplified through the dual-energy decomposition process. The decomposition noise will increase the standard deviation of the measurement in an ROI, but may not significantly affect the mean values in the measurement, as long as a sufficient number of pixels can be included in the ROI. Thus, a reliable characterization of lesion composition may be obtained at a relatively low dose level. However, for very small lesions, the accuracy of lesion characterization may be impaired by the small difference between lesion and normal tissue in the background. A limit of 10 mm was predicted by a previous theoretical study on lesion discrimination.[44] In clinical images, lesions may have irregular shapes. This method measures the integrated signal inside a lesion, followed by the subtraction of the background. Thus it is less sensitive to the shape, but more sensitive to the integrated volume of a lesion.

5. CONCLUSION

In summary, dual-energy material decomposition method was used to characterize lesions in terms of water and lipid in a phantom study with a photon-counting spectral mammography system. The proposed method can accurately quantify the water content with an approximate error of less than 0.4 mm. The results showed that the technique is accurate for different breast thicknesses, densities, and lesion locations. Accurate quantification of breast lesion content can potentially help distinguish between malignant and benign lesions.

ACKNOWLEDGMENTS

This work was supported in part by NIH/NCI Grant No. R01CA13687. Dr. Cho's current working address is Center for Medical Metrology, Division of Convergence Technology, Korea Research Institute of Standards and Science.

CONFLICT OF INTEREST DISCLOSURE

The authors have no COI to report.

[a)]Author to whom correspondence should be addressed. Electronic mail: symolloi@uci.edu; Telephone: (949) 824–5904; Fax: (949) 824–8115.

[1]P. Dean and M. Pamilo, "Large-scale breast cancer screening with mammography: High cancer detection rates combined with a low risk of benign biopsy," Radiology **205**, 10 (1997).
[2]E. Schmitt and B. Threatt, "Effective breast cancer detection with film-screen mammography," J. Can. Assoc. Radiol. **36**, 304–307 (1985).
[3]C. J. D'Orsi, "Early detection of breast cancer: Mammography," Breast Cancer Res. Treat. **18**, S107–S109 (1991).
[4]J. M. Lewin, R. E. Hendrick, C. J. D'Orsi, P. K. Isaacs, L. J. Moss, A. Karellas, G. A. Sisney, C. C. Kuni, and G. R. Cutter, "Comparison of full-field digital mammography with screen-film mammography for cancer detection: Results of 4,945 paired examinations 1," Radiology **218**, 873–880 (2001).
[5]M. Sala, M. Comas, F. Macià, J. Martinez, M. Casamitjana, and X. Castells, "Implementation of digital mammography in a population-based breast cancer screening program: Effect of screening round on recall rate and cancer detection," Radiology **252**, 31–39 (2009).
[6]R. E. Bird, T. W. Wallace, and B. C. Yankaskas, "Analysis of cancers missed at screening mammography," Radiology **184**, 613–617 (1992).
[7]R. A. Hubbard, K. Kerlikowske, C. I. Flowers, B. C. Yankaskas, W. W. Zhu, and D. L. Miglioretti, "Cumulative probability of false-positive recall or biopsy recommendation after 10 years of screening mammography a Cohort study," Ann. Intern. Med. **155**, 481–492 (2011).
[8]H. D. Nelson, K. Tyne, A. Naik, C. Bougatsos, B. K. Chan, and L. Humphrey, "Screening for breast cancer: An update for the us preventive services task force," Ann. Intern. Med. **151**, 727–739 (2009).
[9]Y. Jiang, R. M. Nishikawa, R. A. Schmidt, C. E. Metz, M. L. Giger, and K. Doi, "Improving breast cancer diagnosis with computer-aided diagnosis," Acad. Radiol. **6**, 22–33 (1999).
[10]Y. Wu, M. Giger, K. Doi, C. Vyborny, B. Schmidt, and C. Metz, "Artificial neural networks in mammography: Application to decision making in the diagnosis of breast cancer," Radiology **187**, 81–87 (1993).
[11]R. W. Woods, G. S. Sisney, L. R. Salkowski, K. Shinki, Y. Lin, and E. S. Burnside, "The mammographic density of a mass is a significant predictor of breast cancer," Radiology **258**, 417–425 (2011).
[12]S. Chung, A. Cerussi, C. Klifa, H. Baek, O. Birgul, G. Gulsen, S. Merritt, D. Hsiang, and B. Tromberg, "*In vivo* water state measurements in breast cancer using broadband diffuse optical spectroscopy," Phys. Med. Biol. **53**, 6713–6727 (2008).
[13]D. Hsiang, A. Durkin, J. Butler, B. J. Tromberg, A. Cerussi, and N. Shah, "*In vivo* absorption, scattering, and physiologic properties of 58 malignant breast tumors determined by broadband diffuse optical spectroscopy," J. Biomed. Opt. **11**, 044005–044016 (2006).
[14]B. J. Tromberg, A. Cerussi, N. Shah, M. Compton, A. Durkin, D. Hsiang, J. Butler, and R. Mehta, "Imaging in breast cancer: Diffuse optics in breast cancer: Detecting tumors in pre-menopausal women and monitoring neoadjuvant chemotherapy," Breast Cancer Res. **7**, 279–285 (2005).
[15]A. S. Haka, K. E. Shafer-Peltier, M. Fitzmaurice, J. Crowe, R. R. Dasari, and M. S. Feld, "Diagnosing breast cancer by using Raman spectroscopy," Proc. Natl. Acad. Sci. U. S. A. **102**, 12371–12376 (2005).
[16]E. G. Olmstead, "Mammalian cell water; Physiologic and clinical aspects," Ann. Intern. Med. **65**, 390–392 (1966).
[17]P. C. Johns and M. J. Yaffe, "X-ray characterization of normal and neoplastic breast tissues," Phys. Med. Biol. **32**, 675–695 (1987).
[18]A. Tomal, I. Mazarro, E. M. Kakuno, and M. E. Poletti, "Experimental determination of linear attenuation coefficient of normal, benign and malignant breast tissues," Radiat. Meas. **45**, 1055–1059 (2010).
[19]E. Fredenberg, D. R. Dance, P. Willsher, E. Moa, M. von Tiedemann, K. C. Young, and M. G. Wallis, "Measurement of breast-tissue x-ray attenuation by spectral mammography: First results on cyst fluid," Phys. Med. Biol. **58**, 8609–8620 (2013).
[20]J. L. Ducote and S. Molloi, "Quantification of breast density with dual energy mammography: A simulation study," Med. Phys. **35**, 5411–5418 (2008).
[21]J. L. Ducote and S. Molloi, "Quantification of breast density with dual energy mammography: An experimental feasibility study," Med. Phys. **37**, 793–801 (2010).
[22]S. Molloi, J. L. Ducote, H. Ding, and S. A. Feig, "Postmortem validation of breast density using dual-energy mammography," Med. Phys. **41**, 081917 (10pp.) (2014).
[23]M. Lundqvist, M. Danielsson, B. Cederstroem, V. Chmill, A. Chuntonov, and M. Aslund, "Measurements on a full-field digital mammography system with a photon counting crystalline silicon detector," Proc. SPIE **5030**, 547–552 (2003).
[24]G. K. Yadava, A. T. Kuhls-Gilcrist, S. Rudin, V. K. Patel, K. R. Hoffmann, and D. R. Bednarek, "A practical exposure-equivalent metric for instrumentation noise in x-ray imaging systems," Phys. Med. Biol. **53**, 5107–5121 (2008).
[25]H.-M. Cho, W. C. Barber, H. Ding, J. S. Iwanczyk, and S. Molloi, "Characteristic performance evaluation of a photon counting Si strip detector for low dose spectral breast CT imaging," Med. Phys. **41**, 091903 (10pp.) (2014).
[26]A. S. Wang, D. Harrison, V. Lobastov, and J. E. Tkaczyk, "Pulse pileup statistics for energy discriminating photon counting x-ray detectors," Med. Phys. **38**, 4265–4275 (2011).
[27]H. J. Ding and S. Molloi, "Quantification of breast density with spectral mammography based on a scanned multi-slit photon-counting detector: A feasibility study," Phys. Med. Biol. **57**, 4719–4738 (2012).
[28]A. D. Laidevant, S. Malkov, C. I. Flowers, K. Kerlikowske, and J. A. Shepherd, "Compositional breast imaging using a dual-energy mammography protocol," Med. Phys. **37**, 164–174 (2010).

[29]K. Drukker, F. Duewer, M. L. Giger, S. Malkov, C. I. Flowers, B. Joe, K. Kerlikowske, J. S. Drukteinis, H. Li, and J. A. Shepherd, "Mammographic quantitative image analysis and biologic image composition for breast lesion characterization and classification," Med. Phys. **41**, 031915 (8pp.) (2014).
[30]O. Alonzo-Proulx, A. Tyson, G. Mawdsley, and M. Yaffe, "Effect of tissue thickness variation in volumetric breast density estimation," in *Medical Radiology Diagnostic Imaging*, edited by E. Krupinski (Springer, Berlin/Heidelberg, 2008), Vol. 5116, pp. 659–666.
[31]T. Johnson, H. Ding, and S. Molloi, "Breast density quantification with breast computed tomography (CT): A post-mortem study," Phys. Med. Biol. **58**, 8573–8591 (2013).
[32]H. Cho, H. Ding, N. Kumar, D. Sennung, and S. Molloi, "Calibration phantoms for accurate breast density quantification using dual energy mammography" (unpublished).
[33]E. Fredenberg, M. Lundqvist, B. Cederström, M. Åslund, and M. Danielsson, "Energy resolution of a photon-counting silicon strip detector," Nucl. Instrum. Methods Phys. Res., Sect. A **613**, 156–162 (2010).
[34]M. Åslund, B. Cederström, M. Lundqvist, and M. Danielsson, "Scatter rejection in multislit digital mammography," Med. Phys. **33**, 933–940 (2006).
[35]J. L. Ducote, M. J. Klopfer, and S. Molloi, "Volumetric lean percentage measurement using dual energy mammography," Med. Phys. **38**, 4498–4504 (2011).
[36]H. N. Cardinal and A. Fenster, "An accurate method for direct dual-energy calibration and decomposition," Med. Phys. **17**, 327–341 (1990).
[37]K. Levenberg, "A method for the solution of certain problems in least squares," Q. Appl. Math. **2**, 164–168 (1944).
[38]E. M. Fallenberg, C. Dromain, F. Diekmann, F. Engelken, M. Krohn, J. M. Singh, B. Ingold-Heppner, K. J. Winzer, U. Bick, and D. M. Renz, "Contrast-enhanced spectral mammography versus MRI: Initial results in the detection of breast cancer and assessment of tumour size," Eur. Radiol. **24**, 256–264 (2014).
[39]J. M. Boone, A. L. C. Kwan, J. A. Seibert, N. Shah, K. K. Lindfors, and T. R. Nelson, "Technique factors and their relationship to radiation dose in pendant geometry breast CT," Med. Phys. **32**, 3767–3776 (2005).
[40]F. E. Carroll, J. W. Waters, W. W. Andrews, R. R. Price, D. R. Pickens, R. Willcott, P. Tompkins, C. Roos, D. Page, G. Reed, A. Ueda, R. Bain, P. Wang, and M. Bassinger, "Attenuation of monochromatic x-rays by normal and abnormal breast tissues," Invest. Radiol. **29**, 266–272 (1994).
[41]L. W. Sha, E. R. Ward, and B. Stroy, "A review of dielectric properties of normal and malignant breast tissue," in *Proceedings IEEE SoutheastCon 2002* (IEEE, Columbia, SC, 2002), pp. 457–462.
[42]L. Cockmartin, H. Bosmans, and N. W. Marshall, "Comparative power law analysis of structured breast phantom and patient images in digital mammography and breast tomosynthesis," Med. Phys. **40**, 081920 (17pp.) (2013).
[43]R. E. Hendrick, E. D. Pisano, A. Averbukh, C. Moran, E. A. Berns, M. J. Yaffe, B. Herman, S. Acharyya, and C. Gatsonis, "Comparison of acquisition parameters and breast dose in digital mammography and screen-film mammography in the American College of Radiology imaging network digital mammographic imaging screening trial," Am. J. Roentgenol. **194**, 362–369 (2010).
[44]B. Norell, E. Fredenberg, K. Leifland, M. Lundqvist, and B. Cederstrom, "Lesion characterization using spectral mammography," Proc. SPIE **8313**, 831301 (2012).